

Point defect movement and annealing in collision cascades

K. Nordlund* and R. S. Averback

Materials Research Laboratory, University of Illinois at Urbana-Champaign, Urbana, Illinois 61801

(Received 20 December 1996)

The effect of collision cascades on preexisting point defects in crystalline materials was studied by simulating 5 keV collision cascades in gold, copper, aluminum, platinum, and silicon. The results indicate that collision cascades do not significantly affect interstitials or vacancies outside the liquid core of the cascade, although in the fcc metals the heating of the crystal due to the cascade causes some thermal migration of the interstitials. Within the liquid cascade core, both interstitials and vacancies move towards the center of the molten region when it resolidifies and recombine or cluster there. At elevated temperatures, random jumps of interstitials during the thermal-spike phase can cause significant additional trapping of interstitials in the liquid. In contrast to the annealing effects of preexisting damage in the fcc metals, in silicon the amount of new damage created by a cascade is roughly independent of the number of initial point defects. The difference is attributed to the nature of the bonding in the materials. [S0163-1829(97)05729-9]

I. INTRODUCTION

Ion irradiation methods are of considerable interest in many research and practical applications of materials processing.^{1,2} Since most damage produced in materials during ion irradiation derives from a complex process occurring in collision cascades, much research has been devoted to studying these events.^{3,4} Experimental work has shed some light on this problem; however, owing to the difficulty of resolving defect structures inside materials, these studies have had only limited success. Molecular-dynamics (MD) computer simulation offers an alternative approach,^{3,4} which has proved successful in providing both a qualitative and quantitative description of damage production in solids (see, e.g., Refs. 5–9).

In most of the simulation studies performed so far, the initial state of the lattice in which a collision cascade is initiated has been defect free. However, in practice most ion irradiation-induced cascades are produced in regions which have been previously damaged by implanted ions. Therefore, to understand the effect of prolonged implantation on initially crystalline samples, it is important to know how a cascade affects preexisting defects.

Relatively few studies to date have focused on predamaged sample structures. Sayed *et al.*^{10,11} have studied a few overlapping cascades in Si at energies of the order of a few hundred eV. Gao *et al.*¹² very recently worked on multiple overlapping 400 eV to 5 keV cascades in α -iron (a bcc metal), and Foreman *et al.*¹³ simulated a few 1 keV cascades in Cu with preexisting features like vacancy and interstitial loops. Kapinos and Bacon have studied the effect of high vacancy concentrations on vacancy loop formation in Cu, Ni, and Fe.^{14,15} Both Gao and Foreman report that the preexisting features may be partly annealed when overlapped by a new cascade, a fact well known from experiment.¹⁶

There has been much speculation about the motion of point defects in the heat spike and pressure wave associated with cascades.¹⁷ However, no systematic investigation of these effects has been carried out by molecular dynamics, which is the focus of this work.

We create the point defects in well-defined distributions and follow their motion during the simulations. Although our damage distributions are artificial, they allow us to systematically probe the effect of cascades on defects at different locations. We focus on two crystalline materials of contrasting properties: gold, a dense material with metallic bonding and close-packed fcc crystal structure, and silicon, a covalently bonded material with the relatively loose-packed diamond structure. We also report on simulations of cascades in copper and aluminum to determine whether the differences are due to the atom mass or crystal structure, and in platinum to determine the effect of the melting point. We believe this choice of materials sets the bounds for possible behavior.

The paper is organized as follows. In Sec. II, we present our simulation procedures in detail. In Sec. III, we first present and discuss the results of our simulations for the five elements separately, and then compare their common features and differences.

II. SIMULATION AND ANALYSIS METHODS

A. General principles

In this study we were primarily interested in elucidating defect reactions in collision cascades. Therefore, we set up our simulation conditions in a manner which can be expected to provide an as clear view of the processes involved as possible. The electronic stopping power is neglected, since it is expected to contribute only little to the slowing down of 5 keV self-ions in the materials treated here.¹⁸

The initial temperature of the simulation cell was 0 K in most runs. Since the interstitial in gold migrates very easily even at low temperatures,^{19,20} using a 0 K ambient cell temperature is advantageous for clearly distinguishing what part of the defect motion is due to the collision cascade. Experience in the field shows that the initial state of damage production in collision cascades does generally not differ much at temperatures roughly below 100 K, except possibly for lengths of replacement collision sequences,²¹ which are few in number and not of interest here.

For a straightforward comparison between the different materials, we used similar simulation conditions for all elements. The computational cells had a size of roughly $120 \times 120 \times 120 \text{ \AA}^3$, and contained about 90 000 atoms, which were initially arranged in the proper crystal structure of the material. Periodic boundary conditions were used, and the temperature of the three outermost atom layers was scaled toward 0 K to dissipate excess energy. The downwards scaling factor of the temperature was restricted to be less than 0.1 during a single time step. A linkcell calculation²² and variable time step²³ were also employed to speed up the simulations.

The primary set of runs examined interstitial motion. For these, either 50 interstitials and 50 vacancies or only 50 interstitials were introduced in the cell. The number of defects chosen corresponds roughly to the number of Frenkel pairs which can be expected to form from a previous 20–30 keV cascade in the same region.⁴ The defects were introduced randomly using a Gaussian probability distribution centered at the middle of the simulation cell for vacancies and centered on a spherical cell 35 Å from the middle for interstitials. The width of the distribution σ was 18 Å.²⁴ The runs with these defects distributions are labeled Au 2–5, Si 2–5, Cu 2–3, Al 2–3, and Pt 2–3 in Table I. In other sets of runs, we packed between 20 and 200 defects as close to the cell center as possible (Au 6–9), placed 50–200 defects uniformly in the simulation cell (runs Au 10–15) or used elevated temperatures (Au 16–20).

For all the defect distributions, a minimum distance of 10 Å between defects was used to ensure that defects do not annihilate or form clusters independent of the cascade. Test runs showed this to be important. In all the events, the defects were relaxed for 1 ps before the collision cascade was initiated. In the cases where only interstitials were introduced into the cell, the cell size was relaxed to zero pressure using a pressure control algorithm²⁵ before the initiation of the cascade.

The collision cascades were initiated by giving one of the atoms in the lattice a recoil energy of 5 keV. We chose the initial recoil atom and its recoil velocity direction so that the center of the resulting collision cascade roughly overlapped the preexisting defect structure in the simulation cell. The evolution of the cascades was followed for 50 ps.

B. Recognition of defects

During some of the cascade simulations for Au and Si, a defect analysis routine was run every 20th time step to recognize and follow the motion of interstitials. An approach inspired by the structure-factor analysis in Ref. 26 was used to recognize interstitials and the liquid region. The structure factor P_{st} is calculated for each atom i ,

$$P_{st}(i) = \frac{1}{p_u(i)} \left(\sum_j [\theta_i(j) - \theta_i^p(j)]^2 \right)^{1/2},$$

$$p_u(i) = \left(\sum_j [\theta_i^u(j) - \theta_i^p(j)]^2 \right)^{1/2},$$

where $\theta_i(j)$ is a list of the $n_{nb}(n_{nb}-1)/2$ angles formed between atom i and its n_{nb} nearest neighbors. The number

TABLE I. Some results of the cascade events. The root-mean-square (rms) distance of interstitials from the cell center (Au, Cu, Al, and Pt) or the center of the interstitials (Si) is given for the initial and final distributions of interstitials, based on the Wigner-Seitz cell analysis. Unless otherwise noted, the defects were initially arranged spherically around the center of the cell, as explained in the text.

Element	Event number	Defects (int., vac.)		rms distance (Å)	
		Initial	Final	Initial	Final
Au	1	0, 0	4, 4	-	46.9
	2	50, 0	51, 1	44.7	41.3
	3	50, 50	41, 41	48.7	49.8
	4	50, 50	45, 45	48.7	50.3
	5 ^a	50, 50	39, 39	48.7	54.1
Au ^b	6	20, 0	21, 1	15.1	20.3
	7	50, 0	51, 1	23.9	21.0
	8	200, 0	201, 1	35.2	30.5
	9	20, 20	5, 5	25.5	45.8
Au ^c	10	200, 0	201, 1	58.0	57.0
	11	0, 200	6, 206	-	43.9
	12	200, 200	168, 168	58.2	60.6
	13	100, 100	93, 93	57.8	58.7
	14	50, 50	60, 60	56.4	51.8
	15	50, 50	52, 52	56.4	55.9
Au ^d	16	50, 0	52, 2	45.2	41.2
	17	50, 50	27, 27	48.9	53.6
	18	50, 50	25, 25	48.9	52.1
	19 ^a	50, 50	37, 37	48.9	52.3
	20 ^a	50, 50	39, 39	48.9	51.8
	Si	1	0, 0	84, 94	-
2		50, 0	133, 87	52.7	45.1
3		50, 50	140, 143	50.0	44.0
4		50, 50	154, 160	50.0	41.7
5		50, 50	151, 161	50.0	40.3
Cu	1	0, 0	13, 13	-	38.6
	2	50, 50	50, 50	43.1	44.6
	3	50, 50	48, 48	43.1	41.9
Al	1	0, 0	10, 10	-	21.6
	2	50, 50	41, 41	50.8	50.5
	3	50, 50	43, 43	50.8	50.3
Pt	1	0, 0	6, 6	-	37.6
	2	50, 50	48, 48	46.7	47.8
	3	50, 50	45, 45	48.8	49.6

^aEvent with no cascade at a fixed temperature.

^bDefects packed around the cell center.

^cDefects distributed uniformly in cell.

^dHigh substrate temperature.

n_{nb} is determined from the ideal crystal structure, and is 4 for the diamond structure (Si) and 12 for the fcc structure (Au). $\theta_i^p(j)$ is the distribution of angles in a perfect lattice and $\theta_i^u(j) = j\pi/n_{nb}(n_{nb}-1)/2$ the uniform angular distribution. Before doing the sum over the angles the $\theta_i(j)$ lists are sorted by magnitude.²⁶

By analyzing the structure factor of each atom and its neighbors, combined with a kinetic energy criterion, we were able to recognize interstitials and the liquid region during the simulation.

The motion of interstitials throughout a simulation was followed using an interstitial database which contains histories of all interstitials. When an interstitial structure is recognized during one time step, its position is compared to the position of all interstitial structures recognized during previous time steps. In the new time step, if the new interstitial atom is closer than one lattice constant from one of the previously recognized interstitial structures, it is interpreted to be part of the same interstitial. Otherwise, a new interstitial database entry is created.

The position of each interstitial structure during any given time step is calculated as the average position of all atoms which are part of it. If an interstitial structure becomes part of the liquid zone or has not been seen for at least three interstitial analysis steps, it is discarded from the list of current interstitial structures. Thus, after the simulation the interstitial database will contain information on the positions, lifetime, and movement of all interstitial recognized during the simulation.

Independently of the structure-factor analysis, we performed an analysis of the population of the Wigner-Seitz cell of each perfect lattice atom position for a few time steps in each simulation. Wigner-Seitz cells with more than one atom were interpreted as interstitials and empty cells as vacancies. The numbers of defects obtained for any given time in the Wigner-Seitz and structure-factor methods were in good agreement with each other.

C. Gold

For the MD simulations of gold we employed the gold embedded-atom method (EAM) potential used previously at this laboratory in studies of collision cascades.^{7,20} The universal repulsive potential¹⁸ has been fitted to the potential to realistically describe strong collisions.

The interstitials introduced into the cell were given the (100) fcc dumbbell interstitial structure, which is the lowest-energy interstitial of fcc metals.¹⁹ This interstitial is known to migrate very easily. Experimentally no determination of the migration energy in gold has been achieved.¹⁹ The EAM potential predicts a migration energy of 0.06 eV,²⁰ which is realistic for high-temperature migration where quantum effects are no longer important.

In the automatic interstitial recognition procedure, we evaluated the structure factor P_{st} for the 12 nearest neighbors of each atom. We found that different values of P_{st} could be used to distinguish between crystalline atoms, interstitials, and liquid atoms. By comparing the P_{st} analysis to visual inspection of moving defects, we ensured that the analysis did not lose track of moving interstitials and fine-tuned the recognition criteria to recognize interstitials even in intermediate configurations during migration.

We performed four simulations of 5 keV recoil events in which our interstitial analysis method was used: a reference run in an undamaged gold crystal, two simulations with 50 interstitials and 50 vacancies, and one with only 50 interstitials. Figure 1 shows the initial and final distributions of

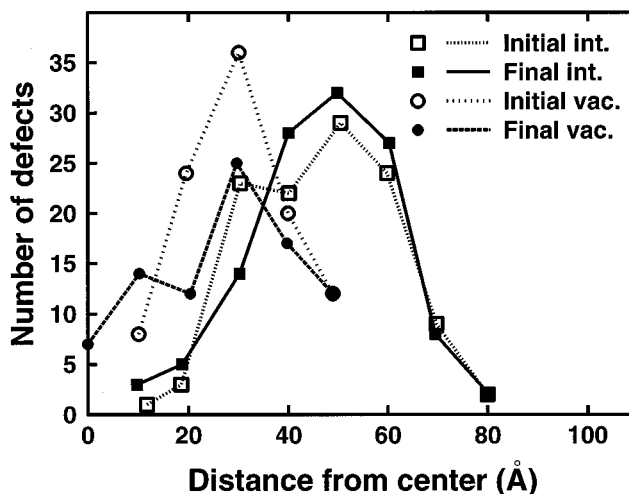


FIG. 1. Distribution of interstitials (int.) and vacancies (vac.) as a function of the distance from the center of the simulation cell before and after the cascade event. The numbers are the sum over the three cascade events discussed in the text. The low number of defects is the reason for the “roughness” of the distributions.

vacancies and interstitials as a function of the distance from the cell center, summed over the three cascade events.

D. Silicon

For realistic MD simulation of covalently bonded materials like silicon, it is important to use an interatomic potential which adequately describes the bonding interactions in the material. We used the Tersoff (C) three-body interatomic potential which gives a good description of several properties of Si, including the different bonding types and elastic moduli.^{27,28} The potential also gives a reasonable description of point defect energies, although the order of the point defect energies is not correct.^{28,29} Since we are primarily interested in the possibility of defect motion, the migration energies of point defects are more significant in any case than their equilibrium structure. Experimental and density-functional results suggest the vacancy migration energy is ~ 0.3 eV.^{30,31} Recent tight-binding molecular-dynamics results give a migration energy of 1.4 eV for the dumbbell interstitial³² (however, in real Si the interstitial migration may be enhanced by defect charge state processes³⁰). For the Tersoff potential, many different values for the interstitial and vacancy migration energies have been reported in the literature, probably due to the difficulty of recognizing the lowest-energy migration path.^{28,33,34} For the vacancy, the lowest migration activation energy calculated for an actual migration path is 1.6 eV,³³ and for the tetrahedral interstitial 1.1 eV.³⁴ Thus, it appears that the Tersoff potential clearly overestimates the vacancy migration energy, but gives a fairly reasonable value for interstitials.

Frequently, the high melting point predicted by the Tersoff potential is used as an argument against its suitability for collision cascade studies. However, using a new reliable approach to calculate the melting point³⁵ we obtained a value of 2300 ± 100 K, which is much less than the conventionally cited value of 3000 K (Refs. 27 and 28) and in better agree-

ment with the experimental value 1685 K.³⁶ Details of this calculation will be given elsewhere.³⁷

A short-range repulsive part of the potential was determined from density-functional theory calculations.^{38,39} It was smoothly fitted to the Tersoff potential using a Fermi function $F(r) = (1 + e^{-b_f(r-r_f)})^{-1}$ with the values 12 \AA^{-1} and 1.6 \AA for b_f and r_f , respectively.⁴⁰ These values provide a smooth fit between the two potentials both between two atoms in a dimer and two nearby atoms in bulk silicon.

The point defect recognition procedure in silicon was similar to the one used in gold. The P_{st} structure factor was evaluated for the four nearest neighbors of each atom, and used to recognize both interstitials and vacancies. Liquid atoms were recognized using a combined P_{st} and kinetic energy criterion.

We carried out 5 simulations for silicon; one reference run with no initial defects, one run with 50 initial interstitials, and three with 50 initial interstitials and 50 initial vacancies.

E. Copper, aluminum, and platinum

For copper, aluminum, and platinum we employed EAM potentials^{41,42} onto which the universal repulsive potential¹⁸ had been fitted to realistically describe strong collisions.²⁶ We carried out 3 simulations for these metals, 1 without initial defects and 2 with 50 initial interstitials and vacancies. The initial defect distributions were the same as for the gold simulations. The analysis of defects was performed with the Wigner-Seitz method for about 20 selected time steps.

III. RESULTS AND DISCUSSION

A. Gold

The gold results will be presented in four subsections. The first deals with defects outside the liquid core of a cascade, the second with defects in the core, the third with uniform defect distributions, and the last one with high-temperature runs.

1. Defects outside the liquid core

Results of one simulation with 50 initial vacancies and interstitials are illustrated in Figs. 2 and 3. Figure 2 shows snapshots of the positions of all atoms in the system projected onto the xy plane at 0, 1.5, and 50 ps. At 0 ps, the initial interstitials and lattice relaxation caused by them are visible among the otherwise undisturbed fcc lattice atoms. At 1.5 ps, we see the liquid cascade center and the pressure wave emanating from it. Some of the interstitials can be discerned even through the pressure wave, showing that they are not destroyed by it. At 50 ps, spike effects are no longer visible, and the lattice has relaxed back close to its initial state. Comparison of the 0 and 50 ps figures shows that most interstitials are positioned at roughly the same sites before and after the cascade. In examining the figures, one should keep in mind that when a dumbbell interstitial is oriented along the z axis, it will not be visible when projected on the xy plane.

Our analysis of interstitial movement enabled us to relate initial and final interstitials to each other. In Fig. 3, the movement of all interstitials which have existed for at least

10 ps (this includes all of the final interstitials) is shown. Most of the interstitials seen in the figure actually existed throughout the simulation. The open markers indicate the initial positions and the solid ones the final positions. The defects move very little during the simulation, even though they clearly have been exposed to the pressure and heat waves from the cascade. Noteworthy is that the interstitials move slightly inwards on average.

These conclusions were verified by a calculation of the total movement of interstitials with respect to the center of mass of the liquid zone throughout the simulation. The interstitials which remained after the cascade had on average moved inwards 1.0, 1.5, and 1.6 \AA in the three cascade events containing preexisting defects. There was, however, a considerable spread in the distribution of the movement: The maximum inwards movement seen in the three events was 10 \AA and the maximum outward movement 14 \AA . On average, the interstitials outside the liquid region performed about three lattice site jumps. From Fig. 1 we see that the overall effect of the interstitial movement on the defect distribution is quite small.

In the events with 50 initial interstitials and vacancies, about 40–45 interstitial structures remained after the cascade event. A few of the interstitials produced in our simulations formed small clusters, but the majority remained as single dumbbell interstitials. Some of the initially existing interstitials have recombined with vacancies during the event. Because this is more likely to occur close to the cell center, the root-mean-square distance of interstitials from the cell center may actually be larger for the final than the initial defect distribution (cf. Table I).

Vacancies were identified geometrically using Wigner-Seitz cells; otherwise, the vacancy analysis employed the same principles as those described above for interstitials. The vacancy movement results are illustrated in Fig. 4. We see that the vacancies outside the liquid region do not move at all or move very little. The average number of lattice site jumps per vacancy was 0.2. This is readily understood in terms of their large migration energy, 0.8 eV.¹⁹

Inspection of animations of the collision cascades showed that most of the interstitial movement occurred when the liquid zone was shrinking in size or had already vanished. To understand the reason for the migration, we calculated temperature and pressure distributions in the cell, which are shown in Figs. 5 and 6. High temperatures are present in the cell for a relatively long period of time after the collision cascade, suggesting this might cause thermal migration of the interstitials. The pressure decreases towards the center of the cell before and after the cascade due to the presence of vacancies near the cell center and the presence of interstitials in the region near the borders (see Fig. 6). We believe this contributes to the inward motion of the interstitials.

In the event which had 50 initial interstitials and no vacancies, a similar pressure gradient was seen, which indicates the interstitials are the predominant cause of it. In the cascade event with no initial defects, in which only four interstitials existed after the cascade, no reduction of the pressure towards the center occurred.

To test whether the defect movement could be explained as a thermal migration process, we simulated the same initial defect distribution as in the cascade events but with no cas-

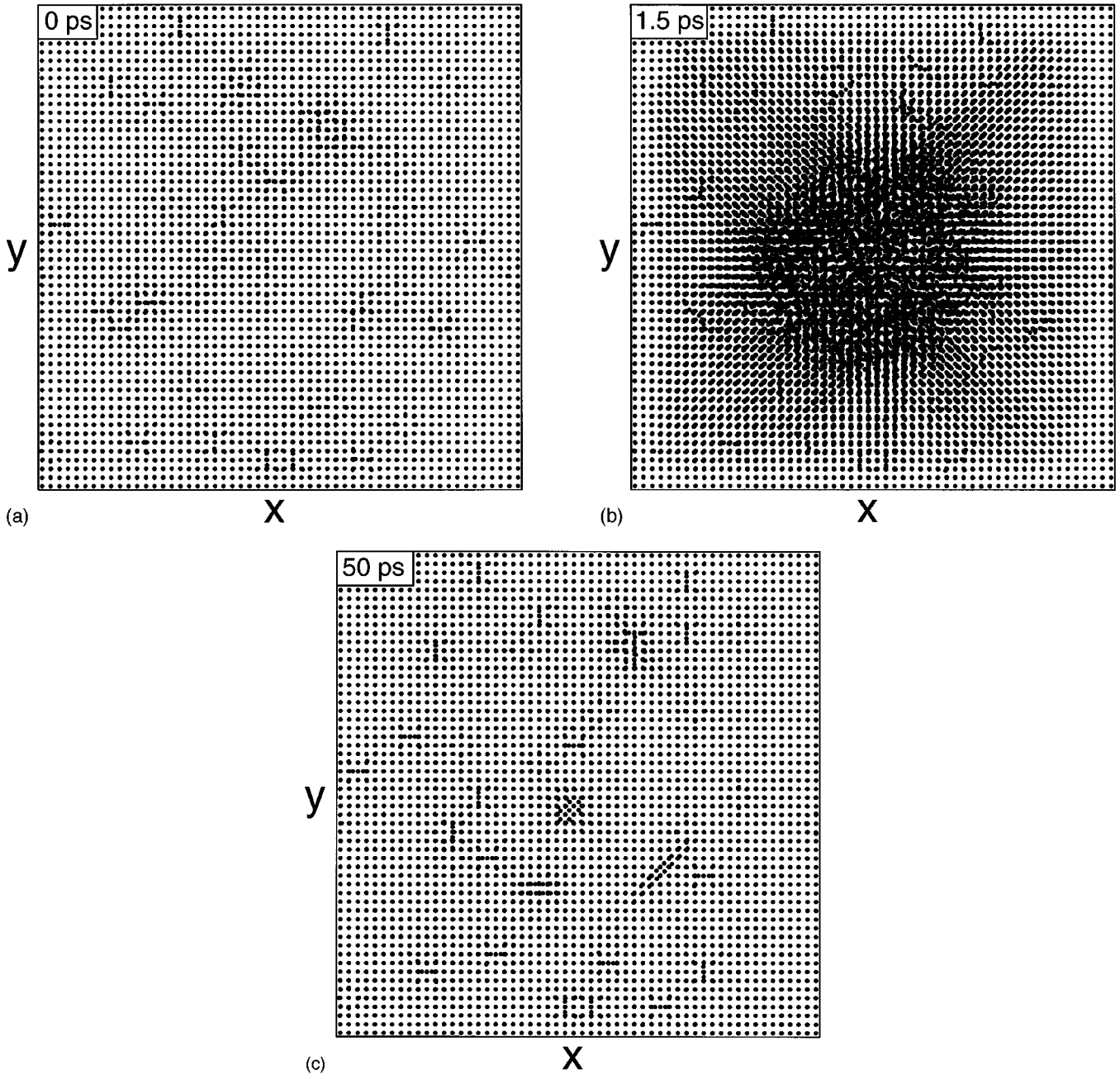


FIG. 2. Snapshots of a 5 keV Au cascade. All atom position in the $(115 \text{ \AA})^3$ simulation cell are included in the figure, projected on the xy plane. The interstitials and lattice relaxation around them breaks the otherwise regular fcc structure in the 0 and 50 ps figures. The liquid zone in the center of the cell and the pressure wave surrounding it can be clearly seen in the 1.5 ps figure. Comparison of the nonregular features in the 0 and 50 ps figures shows that most interstitials have not moved much from their initial positions.

cade initiated in the cell. In case the movement of the interstitials is determined solely by the pressure decreasing inwards and the temperature of the cell, interstitial movement similar to the cascade events should be seen.

A 50 ps simulation was carried out with a cell temperature T_m equivalent to the temperature in the cascade simulations. We assumed the thermal defect migration probability is proportional to $\exp(-E_A/k_B T)$, where $E_A = 0.06 \text{ eV}$.²⁰ Thus the average migration temperature T_m of interstitials is obtained from the temperature of the entire simulation cell as a function of time $T_{\text{casc}}(t)$ in the cascade runs, weighted by the migration exponential,

$$T_m = \frac{\int T_{\text{casc}}(t) e^{(-0.06 \text{ eV})/k_B T(t)} dt}{\int e^{(-0.06 \text{ eV})/k_B T(t)} dt}. \quad (1)$$

From the average of T_m in the three interstitial cascade runs we obtained $T_m = 205 \text{ K}$.

We carried out a 50 ps run for a cell which had 50 interstitials and 50 vacancies distributed as in the cascade runs, but now heating it to 205 K from the borders. We obtained similar results to the cascade runs. Due to the distribution of defects in the cell, the pressure decreased inwards. The interstitials existing after the simulation had, on average, moved 0.6 \AA inwards. As in the case of the interstitials in the

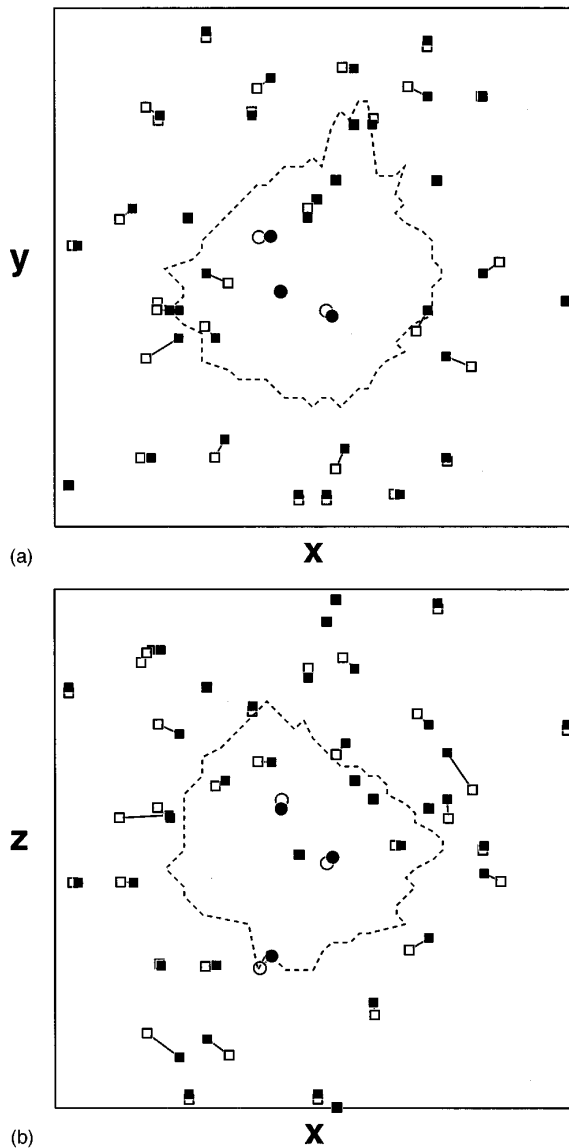


FIG. 3. Movement of interstitials during one 5 keV cascade in gold, projected onto the xy and xz planes. Each marker shows the position of one interstitial (which may contain several atoms). Shown in the figure are all interstitials which have existed for more than 10 ps. Circles show interstitials whose final position is in the zone which at some point of the simulation was liquid, squares other interstitials. The open markers denote the initial positions of the interstitials and the solid markers the final positions. The lines connect the initial and final position of each interstitial. The dashed curve shows the maximum extent of the liquid region.

cascade runs, this average movement was relatively small compared to the random movement in the cell. Since the calculation for T_m includes the liquid core temperature, the number of jumps per interstitial (about 40) and amount of clustering seen in the cell were clearly larger than for the defects outside the liquid core in the cascade events. This indicates that the local temperature has a large effect on the interstitial motion.

During the 50 ps run at 205 K, 11 vacancies annihilated with interstitials. Due to their high migration energy, the rest of the vacancies did not move at all from their initial lattice positions.

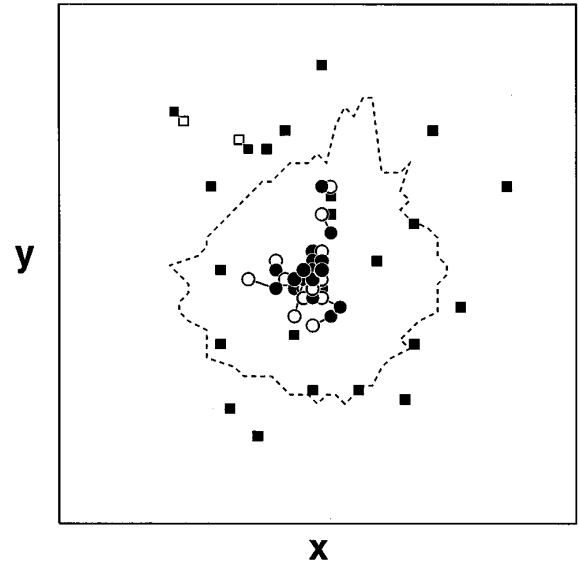


FIG. 4. As Fig. 3, but for vacancies. Circles show vacancies whose final position is in the former liquid zone, squares other vacancies.

The qualitatively similar behavior of the defects in this event and the cascade events indicates that the movement of interstitials adjacent to a collision cascade outside the liquid core can be understood as a thermal migration process. The pressure gradient induced by the nonhomogeneous defect distribution appears to slightly bias the random-walk-like movement of the interstitials.

In conclusion, although the pressure wave emanating from a cascade appears to have little effect on preexisting damage, the high temperatures induced by the cascade can cause some defect migration and annealing outside the liquid core of the cascade.

2. Defects in the liquid core

In the cascade events with spherical defect distributions (Au 2–4), between 10 and 20 initial vacancies and 0 and 5

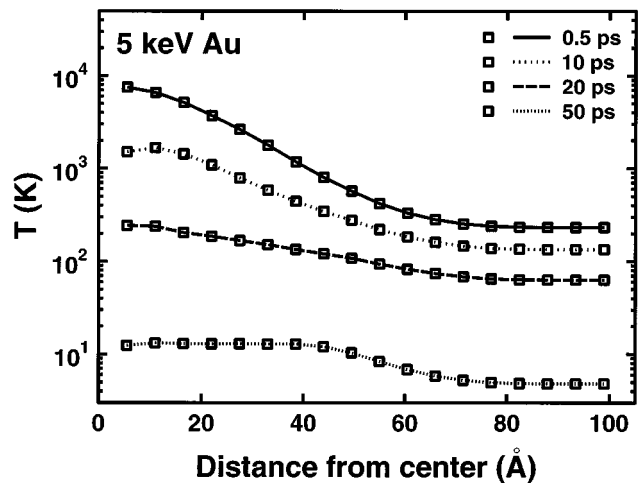


FIG. 5. Temperature at different times in a 5 keV gold cascade as a function of the distance from the cascade center. The temperature at a certain distance is the temperature of all atoms within this distance from the center of the cell.

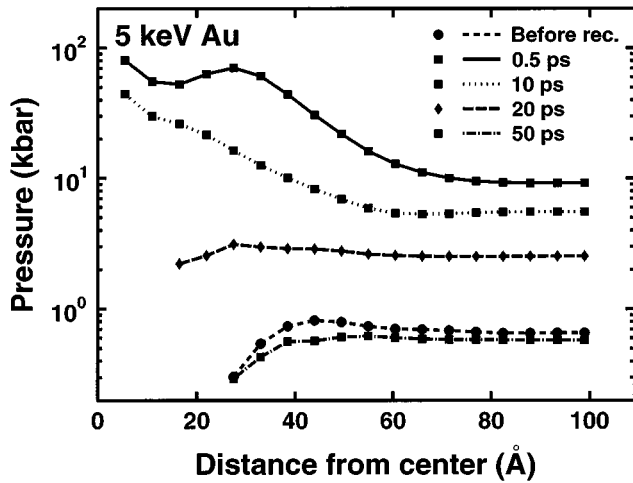


FIG. 6. Pressure as a function of time in a 5 keV gold cascade as a function of the distance from the cascade center, evaluated similarly as the temperature. The initial very high values are caused by the strong collisions in the heart of the cascade. Near the end of the cascade the pressure decreases towards the center of the cell due to the presence of vacancies near the center.

initial interstitials were within the region of the cell which was liquid at some point of the cascade evolution. The volume of the liquid core (defined as the total volume of unit cells which contained liquid atoms at any time during the simulation) was about 4% of the total volume or 4000 atomic volumes.

As shown in Fig. 4, the vacancies within the liquid core of the cascade cluster near the center of the cell. Similar behavior was seen in the two events where preexisting vacancies were placed near the center of the simulation cell. The clustering in the center shows how the crystal regenerative process favors the production of defect-free fcc lattice on resolidification. Since the central region contains too few atoms to form a perfect lattice, a vacancy cluster remains in the center. This result is similar to the copper cascade results of Kapinos and Bacon, which show clustering and loop formation of vacancies in samples with high initial vacancy concentrations.¹⁴

In the event with no initial vacancies (Au 2), 12 of the 50 initial interstitials got trapped in the liquid region and formed an interstitial cluster in the center it. This shows that the resolidification kinetics is sufficiently fast to avoid quenching in defects and that the high-pressure gradient in the core of a cascade does not push the interstitials outwards, as might be expected. This is discussed further in Sec. IIIA4.

We also tested the behavior of interstitials near the cascade core. We simulated three 5 keV Au cascade events in which the cell contained 20, 50, and 200 interstitials, placed spherically around the center of the cell using the 10 Å minimum distance between defects (runs Au 6–8 in Table I). No vacancies were included in the initial cell in these events.

In these cascades, the final cell contained 21, 51, and 201 final interstitials, and a single vacancy in each case. The interstitials formed large clusters in all events, although a few isolated interstitials were seen as well. In reference events where a 5 keV event was simulated in an undisturbed fcc lattice typically around 5 vacancies and interstitials were

produced in the cascade. The fact that very few vacancies were seen even in the 20 interstitial event indicates that the presence of preexisting interstitials inhibits the creation of vacancies in a collision cascade; i.e., vacancies and interstitials cannot coexist in the liquid core. Again, interstitial clusters were observed in the center of the cascade.

We also simulated one event (run Au 9) in which we placed 20 interstitials and 20 vacancies as close to the center of the cell as possible while retaining the 10 Å minimum distance between them. After a 5 keV cascade event there were 5 interstitials and 5 vacancies left in the cell, confirming that damage anneals in the liquid core of the cascade. The surviving interstitials were located far away from the cascade center, whereas 4 of the vacancies were close to the center.

3. Uniform defect distributions

In the events described above, the final amount of damage was generally reduced by a cascade, but the effect was strongly dependent on the shape of the (somewhat artificial) initial defect distributions. To provide an estimate of what defect concentration is large enough to cause a reduction of the final number of defects, we simulated a number of events with a uniform defect concentration in the simulation cell (the defects were introduced in the cell on random atom sites). The numbers of initial and final defects in these events are listed in Table I as events Au 12–15.

For 200+200 and 100+100 initial interstitials and vacancies the number of defects decreases as a result of a 5 keV cascade, whereas for 50+50 initial defects the number increases. Considering only the defect-producing and annealing effect of the 5 keV cascades described above, we obtain that the equilibrium number of defects is of the order of 1×10^{-3} . This result corresponds closely to experiments in which defects were introduced randomly by proton irradiation and subsequently annealed by heavy ion irradiation.¹⁶

In a cascade event (run Au 10) with a large number of randomly distributed initial interstitials, only one vacancy is created, in good agreement with our earlier observation that interstitials appear to inhibit vacancy production. On the other hand, in run Au 11 which had a large number of initial vacancies, six interstitials were produced, indicating that the opposite is not necessarily true. This reflects the fact that newly produced interstitials are ejected from the liquid and avoid recombination, whereas vacancies are always produced in the liquid.

4. Damage at 600 K

Since most practical ion irradiations are performed at temperatures much higher than 0 K, we performed a few simulations at 600 K (runs Au 16–19). The initial defect distributions were the same as in runs Au 2–5. Prior to the initiation of a the cascade, the pressure in the cell was equilibrated to 0 kbar and the atoms were given realistic thermal displacements by performing a 5 ps run at 600 K using a variable cell size and a pressure control algorithm.²⁵

To check how many defects annihilate due to thermal motion alone, two 50 ps runs were performed at a fixed temperature with no cascade in the cell. Run Au 19 was performed at 600 K and run Au 20 at 670 K [the average

cascade temperature evaluated using Eq. (1)] The 600 and 670 K runs resulted in the annihilation of 13 and 11 defects, respectively.

In the two cascade events with 50 initial vacancies and interstitials, the number of defects after the cascade was about 25 and 27, which is 15–20 less than in the 0 K events. Inspection of animations of the cascades showed that most of the defects vanished in the early part of the cascade, in less than 20 ps. Since thermal migration processes account for only around 10 recombinations of defects, there must be another defect annealing mechanism active. Since the volume of the liquid region was only about 30% larger at 600 K than at 0 K, it cannot have reached very many more interstitials than in the 0 K runs.

The liquid region recrystallized much slower than in the 0 K runs; parts of the liquid remained even after 20 ps, and its maximum volume was slightly bigger. We know from our earlier work that a fcc interstitial jumps about once every 2 ps at 600 K.⁴³ At the elevated temperatures close to the core of the cascade, the interstitials can be expected to make more than 10 jumps in 20 ps. Thus, at elevated temperatures interstitials on the periphery of the melt zone can migrate to it before it contracts on resolidification. These interstitials recombine with vacancies in the melt, reducing the number of defects.

In the event with 50 initial interstitials and no vacancies, 22 of the interstitials got trapped in the liquid and formed a cluster in its center. Since an interstitial has a high formation energy in the crystal, but essentially none in a liquid, it is unlikely that an interstitial which has entered the liquid leaves it again. With no vacancies in the cell, the interstitials therefore have to move with the liquid to its center, explaining the cluster formation.

At lower temperatures the interstitials move much more slowly and the melt contracts before the interstitials reach it. Since the vacancies are drawn to the center of the cascade, as we have shown above, interstitials and vacancies become well separated: Subsequent motion of the interstitials then allows them to escape without recombination. Recent work by Daulton *et al.* shows, in fact, that vacancy retention in cascades decreases rapidly with temperatures above about 300 °C.⁴⁴ The authors say this cannot be explained by dissolution of the vacancy clusters. We believe the mechanism found here can explain their result.

To conclude the gold results, we have identified three damage annealing mechanisms by collision cascades in gold. Interstitial and vacancies can recombine during thermal migration caused by the heating of the crystal by the cascade. Defects captured in the liquid formed by the cascade are likely to be forced into the liquid center during the collapse of the liquid, and recombine or (if equal numbers of vacancies and interstitials are not present in the liquid) form clusters there. Finally, at increasing temperatures the random motion of interstitials makes them increasingly likely to reach the liquid because of their thermal migration, increasing damage annealing.

We find similar behavior for other fcc metals, presented in Sec. IIIC below. The α -iron results of Gao *et al.*¹² show that the amount of damage in multiple overlapping cascades saturates. For high-energy cascades they offer two explanations for this: defect loss in the cascade core and defect loss due to

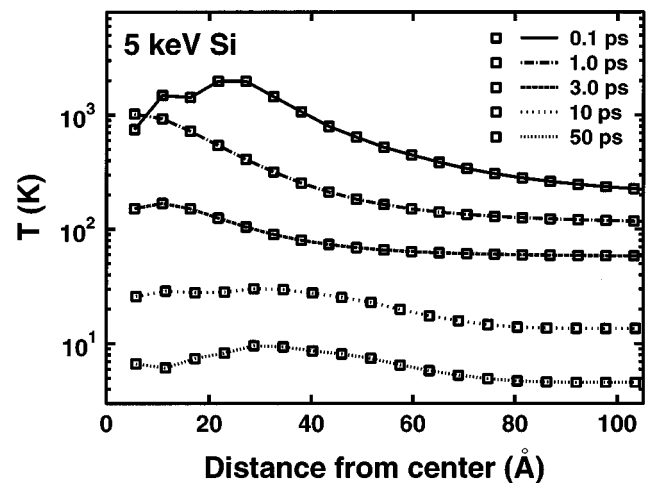


FIG. 7. As Fig. 5, but for silicon.

increased migration induced by the heating of the cell, which are essentially the same mechanisms found by us for low-temperature cascades in gold. It appears that these damage annealing mechanisms are significant in several different types of metals.

B. Silicon

The silicon results differed dramatically from those in gold. No statistically significant motion of interstitials or vacancies was observed outside the liquid core of the cascade (the number of site jumps per defect was less than 0.1). We attribute this to the high migration energies of an interstitial and vacancy in Si. Also, the Si cascade cools down much faster than the Au one (compare Figs. 5 and 7). As in gold, the heat and pressure waves from the cascade do not appear to have any effect on the defects.

The 5 keV cascade run in an undamaged lattice created 84 interstitials and 90 vacancies, counted using the Wigner-Seitz cell analysis; the structure factor analysis typically gave about 10–20 % smaller numbers of defects. Some of the Wigner-Seitz cells contain more than 2 atoms, explaining why the number of interstitials and vacancies are not equal. The number of atoms with a potential energy more than 0.2 eV higher than that of undisturbed lattice atoms was found to be 910. This agrees well with the results of Díaz de la Rubia and Gilmer,⁵ who found about 800 final defect atoms with the same criterion in a 5 keV Si cascade using the Stillinger-Weber potential.⁴⁵ This indicates that the Tersoff and Stillinger-Weber potentials yield similar results in simulations of collision cascades.

The number of defects produced in the runs with initial defects are shown in Table I. We see that a 5 keV cascade in silicon creates roughly 100 interstitials and vacancies, regardless of the initial distribution of point defects in the simulation cell. This is in clear contrast to the results in gold, in which the initial and final number of defects were slightly reduced from the initial number. It is evident that the crystal regeneration effect present in the collapse of the collision cascade in gold is absent in silicon. Furthermore, about 10 of the initial interstitials and vacancies are within the liquid zone of the cascade (the total volume of which encompasses

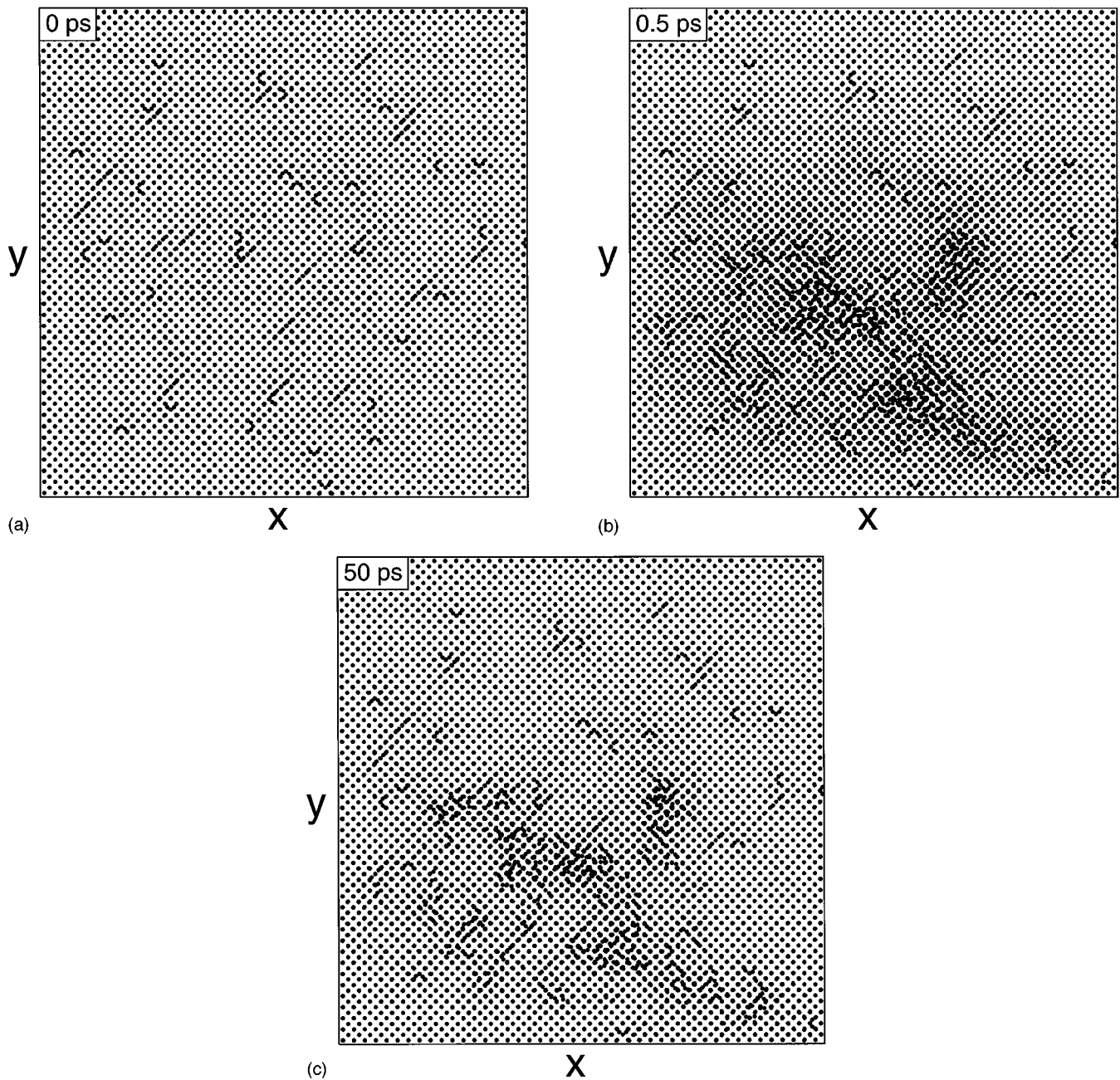


FIG. 8. As Fig. 2, but for Si. The cascade is clearly less dense and well defined than in gold, and much more damage remains afterwards.

about 3% of the cell volume). In case the liquid part of the cascade would have an annealing effect on defects in it, the number of new defects produced in a defect cell should be smaller than for an event in a virgin cell. However, the numbers obtained appear to be equal or even larger.

Thus, no sign of an annealing effect in the Si cascades can be seen; instead the preexisting damage, if it has any effect at all, enhances damage production. This is in good agreement with the experimental observation that the fraction of amorphous material can increase superlinearly with dose during ion irradiation.^{5,46,47}

The initial, “peak of the cascade” and final atom positions of the event with both initial vacancies and interstitials are shown in Fig. 8. Analysis of the damage in the events showed that all of the new defects are created in the liquid

zone of the cascade region. The damage takes the form of complex clusters and amorphous pockets, similar to those seen in the work of Díaz de la Rubia and Gilmer.⁵ As they already have studied the nature of such damage in single cascades in some detail, we do not discuss it here.

C. Copper, aluminum and platinum

Since Cu and Al have the same metallic bonding and fcc crystal structure as gold, but a mass closer to that of Si, the simulations of cascades in Cu and Al enabled us to determine whether the difference in the Si and Au results was due to the mass or crystal structure difference. Similarly, comparison of the gold and platinum results probes the effect of

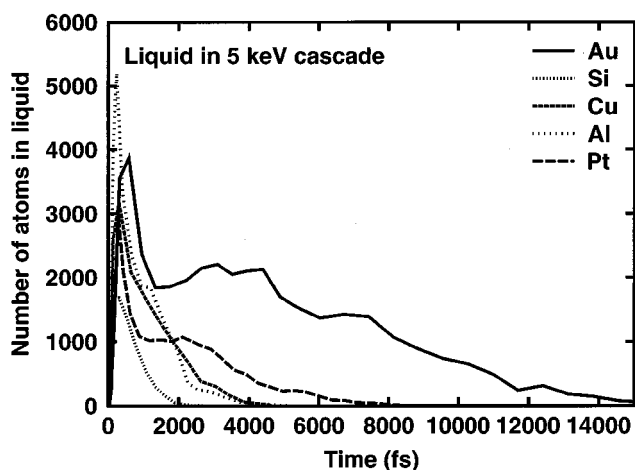


FIG. 9. Number of liquid atoms as a function of time in five 5 keV cascade events. Comparison of different events showed that the results do not differ much between events in the same element.

the melting point, as gold and platinum have practically the same mass, but the melting points are 1480 K and 1090 K in the EAM formalism.²⁰

The defect production and annealing results obtained in Cu, Al, and Pt were remarkably similar to the results in Au (see Table I). Although the cascades in the two metals, and particularly in Al, were clearly less dense than the cascades in Au, the effect on the number defects was roughly the same. In all runs with 50 initial interstitials and vacancies, the final number of defects varied between 40 and 50.

D. Comparison of metals and silicon

The results presented above have shown that the nature of the damage produced and the effect of a cascade on preexisting damage differ dramatically in fcc metals and in silicon. The metal results were obtained with four different EAM potentials, and the amount of damage produced in our Si simulations carried out with the Tersoff potential agrees well with results obtained using the Stillinger-Weber potential. Therefore, we do not consider it likely that the metal-silicon difference is an artifact of the simulation methods or potentials used. The fcc results are very similar to each other, and so the difference in the results appears to be caused by some fundamental difference between fcc metals on the one hand and silicon on the other.

The melting point of silicon with the present potential is 2300 K, and the melting points of the metals vary between 900 and 1500 K.²⁰ Since silicon has a higher melting point than the fcc metals, this could explain part of the difference. Figure 9, however, shows that even though the number of liquid atoms is clearly the lowest in silicon, qualitatively the Si and Cu/Al cooling curves are similar. Also, although the number of liquid atoms in Pt is clearly less than that in Au, due to the large difference in melting points, the number of defects produced and/or annealed in both Au and Pt is very similar.

Damage production and annealing in all the fcc metals appears to be very similar despite their large differences in mass. On the other hand, the difference between the Si and

Al results is large despite their negligible difference in mass. This shows that mass differences are not a very significant factor in damage production.

From the above discussion, it appears clear that differences in the melting points and cooling rates do not affect damage production and annealing behavior much in materials with the same crystal structure. We attribute the differences to the crystal structure and bonding type. The close-packed fcc crystal structure strongly favors regeneration into the perfect structure, making it easy to anneal preexisting point defects in the sample. The results of Foreman *et al.*¹³ show that a cascade can separate complex damage like defect loops into smaller damage structures. This effect combined with the point defect annealing mechanisms observed in the present work can, at least qualitatively, explain the experimental observation that damage levels in pure metals saturate during prolonged implantation.¹⁶

The relatively open diamond structure, on the other hand, can incorporate numerous complex defect structures, and silicon can form nontetrahedral covalent bonds which are not too much higher in energy than tetrahedral bonding.²⁷ This makes defect annealing significantly slower in Si than in the metals and apparently not possible during the short time scales present in cascades.

IV. CONCLUSIONS

In this paper we have studied how a collision cascade affects preexisting damage in solids having different characteristics. At low temperatures, we showed for both gold and silicon that the pressure and heat waves emanating from a collision cascade do not directly cause any significant motion of defects outside the liquid core of the cascade. However, in gold the heating of the crystal due to the cascade does cause some thermal movement of interstitials existing outside the liquid core of the cascade.

In fcc metals, we demonstrated that both interstitials and vacancies are pushed toward the center of the liquid region when the molten region resolidifies. We identified three mechanisms of damage annealing by collision cascades. The thermal movement of interstitials outside the liquid core of the cascade may cause some of them to recombine with vacancies. Defects captured in the liquid formed by the cascade are likely to be forced into the liquid center during the collapse of the liquid and recombine there. At high temperatures the random motion of interstitials makes them likely to reach the liquid zone of a cascade, increasing the number of defects captured and recombining in the melt. In cases where the defect numbers in the liquid are not equal, the latter two processes result in clustering of residual defects in the center of the molten region.

The damage annealing mechanisms identified in this study were used to explain experimental data on damage produced during ion irradiation.

For silicon, we found that the amount of new damage produced in a cascade is the same or somewhat increased in samples with preexisting point defects as in undamaged samples. The damage produced was of a complex nature, and produced exclusively in or adjacent to the core of the cascade.

From a comparison of results in the fcc metals Al, Cu, Pt,

and Au, and the results in the diamond-structured Si, we attributed the difference in damage production in the two kinds of solids to be due to the nature of bonding.

ACKNOWLEDGMENTS

We are thankful to Dr. T. Díaz de la Rubia and Dr. M. Ghaly for useful discussions during the course of this work.

The research was supported by the U.S. Department of Energy, Basic Energy Sciences under Grant No. DEFG02-91ER45439, and by the Academy of Finland and University of Helsinki. Grants of computer time from the National Energy Research Computer Center at Livermore, California, the National Center for Supercomputing Applications, and the Materials Research Laboratory at the University of Illinois at Urbana-Champaign are gratefully acknowledged.

- *Permanent address: Accelerator Laboratory, P.O. Box 43, FIN-00014 University of Helsinki, Finland. Electronic address: kai.nordlund@helsinki.fi
- ¹J. Asher, Nucl. Instrum. Methods Phys. Res. B **89**, 315 (1994).
 - ²C. Jaussaud, J. Margail, J. Lamure, and M. Bruel, Radiat. Eff. Defects Solids **127**, 319 (1994).
 - ³R. S. Averback, J. Nucl. Mater. **216**, 49 (1994).
 - ⁴D. J. Bacon and T. Diaz de la Rubia, J. Nucl. Mater. **216**, 275 (1994).
 - ⁵T. Diaz de la Rubia and G. H. Gilmer, Phys. Rev. Lett. **74**, 2507 (1995).
 - ⁶K. Nordlund, J. Keinonen, E. Rauhala, and T. Ahlgren, Phys. Rev. B **52**, 15 170 (1995).
 - ⁷M. Ghaly and R. S. Averback, Phys. Rev. Lett. **72**, 364 (1994).
 - ⁸H.-P. Kaukonen and R. M. Nieminen, Phys. Rev. Lett. **68**, 620 (1992).
 - ⁹I. Kwon, R. Biswas, G. S. Grest, and C. M. Soukoulis, Phys. Rev. B **41**, 3678 (1990).
 - ¹⁰M. Sayed, J. H. Jefferson, A. B. Walker, and A. G. Gullis, Nucl. Instrum. Methods Phys. Res. B **102**, 218 (1994).
 - ¹¹M. Sayed, J. H. Jefferson, A. B. Walker, and A. G. Gullis, Nucl. Instrum. Methods Phys. Res. B **102**, 232 (1994).
 - ¹²F. Gao *et al.*, J. Nucl. Mater. **230**, 47 (1996).
 - ¹³A. J. E. Foreman, W. J. Phythian, and C. A. English, Radiat. Eff. Defects Solids **129**, 25 (1994).
 - ¹⁴V. G. Kapinos and D. J. Bacon, Phys. Rev. B **53**, 8287 (1996).
 - ¹⁵V. G. Kapinos and D. J. Bacon, Phys. Rev. B **52**, 4029 (1995).
 - ¹⁶R. S. Averback, J. Nucl. Mater. **108&109**, 33 (1982).
 - ¹⁷D. J. Bacon, in *Computer Simulation in Materials Science*, Vol. 3–8 of *NATO ASI Series E: Applied Sciences*, edited by H. O. Kirchner, L. P. Kubin, and V. Pontikis (Kluwer Academic Publishers, London, 1995), p. 189, and references therein.
 - ¹⁸J. F. Ziegler, J. P. Biersack, and U. Littmark, *The Stopping and Range of Ions in Matter* (Pergamon, New York, 1985).
 - ¹⁹P. Ehrhart, K. H. Robrock, and H. R. Shober, in *Physics of Radiation Effects in Crystals*, edited by R. A. Johnson and A. N. Orlov (Elsevier, Amsterdam, 1986), p. 3.
 - ²⁰M. S. Daw, S. M. Foiles, and M. I. Baskes, Mater. Sci. Rep. **9**, 251 (1993).
 - ²¹F. Gao and D. J. Bacon, Philos. Mag. A **71**, 43 (1995).
 - ²²M. P. Allen and D. J. Tildesley, *Computer Simulation of Liquids* (Oxford University Press, Oxford, England, 1989).
 - ²³K. Nordlund, Comput. Mater. Sci. **3**, 448 (1995).
 - ²⁴In practice, the final defect distributions were somewhat distorted from the ideal Gaussian shape due to the use of the 10 Å minimum distance criterion.
 - ²⁵H. J. C. Berendsen *et al.*, J. Chem. Phys. **81**, 3684 (1984).
 - ²⁶H. Zhu, R. S. Averback, and M. Nastasi, Philos. Mag. A **71**, 735 (1995).
 - ²⁷J. Tersoff, Phys. Rev. B **38**, 9902 (1988).
 - ²⁸H. Balamane, T. Halicioglu, and W. A. Tiller, Phys. Rev. B **46**, 2250 (1992).
 - ²⁹R. Car, P. Blochl, and E. Samrgiassi, Mater. Sci. Forum **83-87**, 433 (1992).
 - ³⁰M. Lannoo and J. Bourgoin, *Point Defects in Semiconductors* (Springer, Berlin, 1981).
 - ³¹P. J. Kelly, R. Car, and S. T. Pantelides, Mater. Sci. Forum **10-12**, 115 (1986).
 - ³²M. Tang, L. Colombo, J. Zhu, and T. Diaz de la Rubia, Phys. Rev. B **55**, 14 279 (1997).
 - ³³M. Kitabatake and J. E. Greene, J. Appl. Phys. **73**, 3183 (1993).
 - ³⁴P. J. Ungar, T. Takai, T. Halicioglu, and W. A. Tiller, J. Vac. Sci. Technol. A **11**, 224 (1996).
 - ³⁵J. R. Morris, C. Z. Wang, K. M. Ho, and C. T. Chan, Phys. Rev. B **49**, 3109 (1994).
 - ³⁶J. W. Mayer and S. S. Lau, *Electronic Materials Science For Integrated Circuits in Si and GaAs* (MacMillan, New York, 1990).
 - ³⁷J. P. Pulkkinen, A. Kuronen, J. Keinonen, and K. Nordlund (unpublished).
 - ³⁸J. Keinonen *et al.*, Nucl. Instrum. Methods Phys. Res. B **88**, 382 (1994).
 - ³⁹K. Nordlund, N. Runeberg, and D. Sundholm (unpublished).
 - ⁴⁰K. Nordlund, J. Keinonen, and T. Mattila, Phys. Rev. Lett. **77**, 699 (1996).
 - ⁴¹M. J. Sabochick and N. Q. Lam, Phys. Rev. B **43**, 5243 (1991).
 - ⁴²A. Voter and S. P. Chen, in *Characterization of Defects in Materials*, edited by R. W. Siegel, J. R. Weertman, and R. Sinclair, MRS Symposia Proceedings No. 12 (Materials Research Society, Pittsburgh, 1987), p. 175.
 - ⁴³H. Zhu and R. S. Averback (unpublished).
 - ⁴⁴T. L. Daulton, M. A. Kirk, and L. E. Rehn in *Materials Modification and Synthesis by Ion Beam Processing*, edited by D. E. Alexander, N. W. Cheung, B. Park, and W. Skorupa, MRS Symposia Proceedings No. 438 (Materials Research Society, Pittsburgh, in press).
 - ⁴⁵F. H. Stillinger and T. A. Weber, Phys. Rev. B **31**, 5262 (1985).
 - ⁴⁶O. W. Holland, J. Narayan, and D. Fathy, Nucl. Instrum. Methods Phys. Res. B **7/8**, 243 (1985).
 - ⁴⁷G. Bai and M.-A. Nicolet, J. Appl. Phys. **70**, 649 (1991).